

Experimental study of katabatic jets over steep slopes: buoyancy effect on turbulence and first insight on slope-normal velocity

Claudine CHARRONDIÈRE

Christophe BRUN and Martin OBLIGADO

Laboratoire des Ecoulements Géophysiques et Industriels (LEGI, Grenoble, France)

Jean-Martial COHARD, Catherine COULAUD and Hélène GUYARD
Institut des Géosciences de l'Environnement (IGE, Grenoble, France)

Jean-Emmanuel SICART and Romain BIRON
Institut de Recherche pour le Développement (IRD, Grenoble, France)



Context and stakes

Transport and storage of pollutants in valleys

Whiteman D (2000)

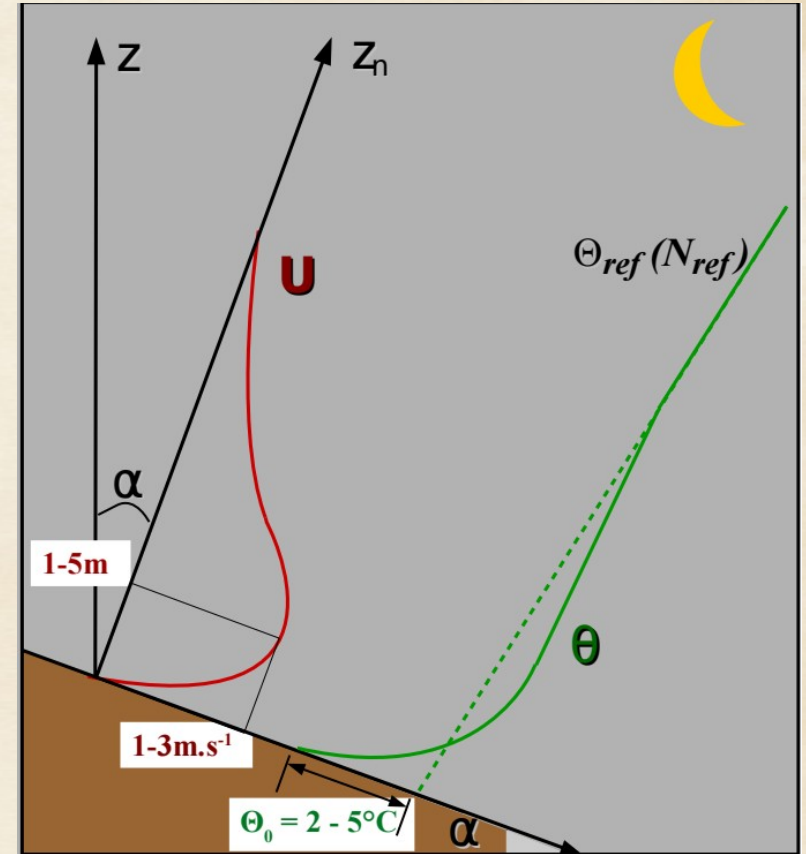
Largeron Y, Staquet C (2016)

Parameterization of katabatic flows and turbulence in meteorological models

Blein S (2016)



Valley of Grenoble viewed from the measurement site – February 2019



Katabatic jet: gravity flow that develops in stably stratified conditions, due to a negative surface energy balance (often during nighttime)

2012 November field experiment

- * Presentation of the field campaign
- * Buoyancy effect on turbulence kinetic energy (TKE)
- * Buoyancy effect on turbulent shear stress $\overline{u'w'}$

2019 February field experiment

- * Presentation of the field campaign
- * Improvements from the 2012 experiment
 - Tethered balloon above the mast and background stratification
 - Time-resolved measurements close to the ground ($f=1250\text{Hz}$)
 - Measurement of entrainment / detrainment in mean velocity profiles

2012 November field experiment

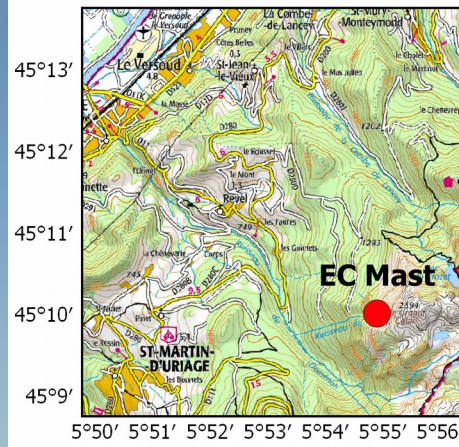
$z_n = 6.31\text{m}$

6.5 m high mast

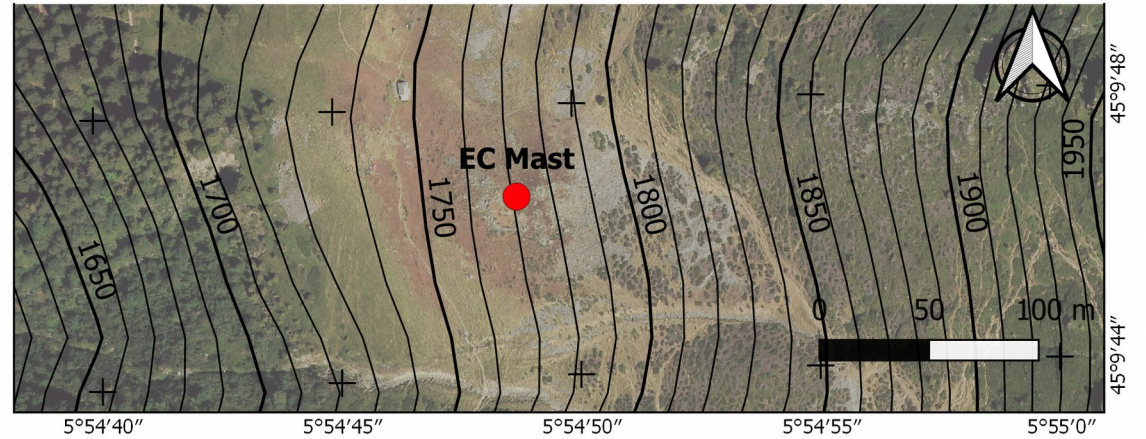
$z_n = 3.98\text{m}$

$z_n = 1.77\text{m}$

$z_n = 1\text{m}$



Belledonne mountain range (French Alps)



Slope angle $\alpha = 21^\circ$ (streamline)

Anticyclonic conditions

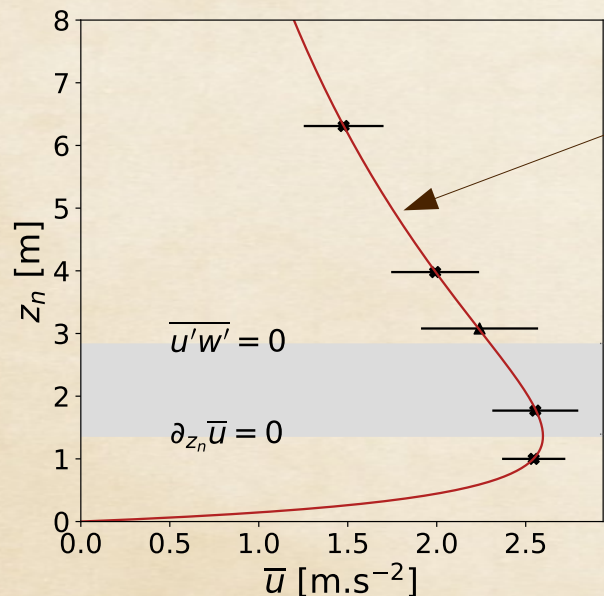
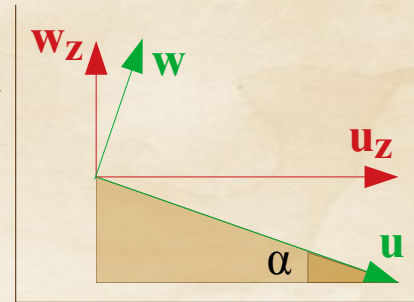
Brünt-Väisälä frequency $N \sim 0.02\text{Hz}$

Reynolds decomposition with $\tau = 2$ min:

$$a(t) = \overline{a} + a'(t)$$

- 4 3D sonic anemometers (10-20 Hz)
- 1 2D sonic anemometer (0.5Hz)
- 1 thermo-hygrometer
- 1 infrared-thermometer

Pure katabatic event : 2012 November 19th (1915-1945 Local Time)



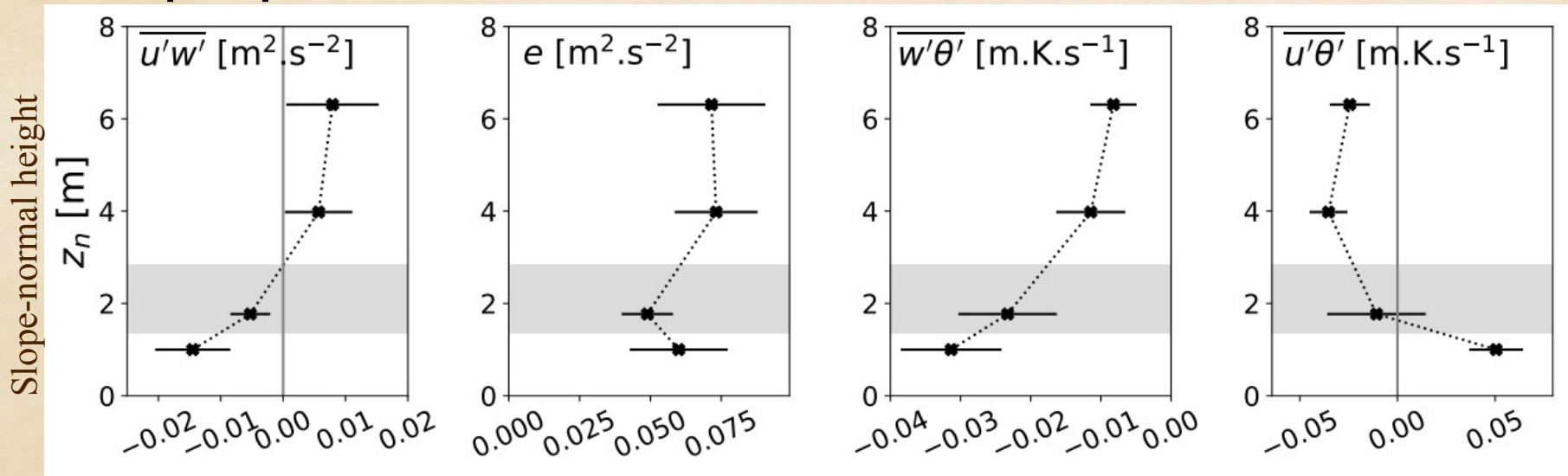
Prandtl model with varying eddy-diffusivity coefficients
 $Km(z_n)^{1,2}$:

$$\bar{u}(z_n) = V_0(z_n) \cdot \sin \frac{z_n}{L_0(z_n)} \cdot e^{\frac{-z_n}{L_0(z_n)}}$$

Outer layer : turbulent shear layer
 $u'w' > 0$

Region of the maximum of wind speed

Inner layer region : turbulent boundary layer
 $u'w' < 0$



1. Grisogono et al. (2001), J Atmos Sci 58(21):3349–3354 / 2. Brun et al. (2017), J Atmos Sci 74(12):4047–4073

Charrondiere et al. (2020), Boundary-Layer Meteorol (Under review)



Buoyancy effect on turbulence kinetic energy

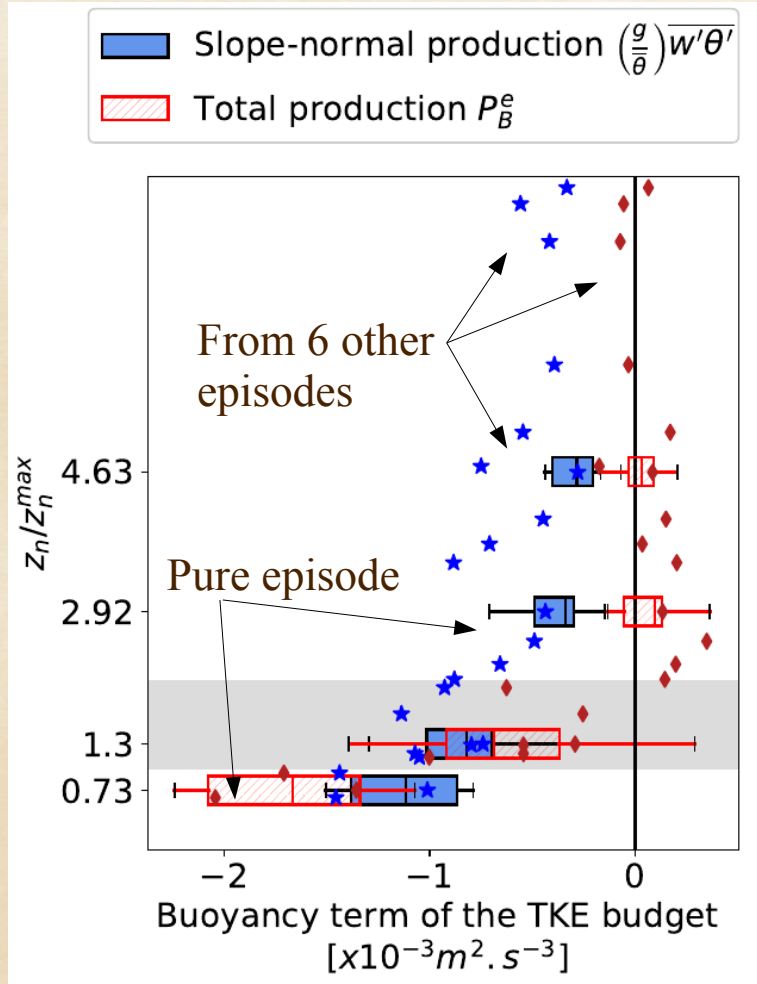
Turbulence kinetic energy (TKE)

$$e = 0.5 (\overline{u'^2} + \overline{v'^2} + \overline{w'^2})$$

Buoyancy term in the TKE budget

$$P_B^e = \frac{g}{\theta} \cdot \overline{w'_z \theta'} = \frac{g}{\theta} \cdot (\overline{w' \theta'} \cos \alpha - \overline{u' \theta'} \sin \alpha)$$

Slope-normal height normalized by the maximum wind speed height



Production of TKE

Consumption of TKE

Consumption of TKE

Slope effect

Consumption of TKE

Production
(limited consumption)
of TKE

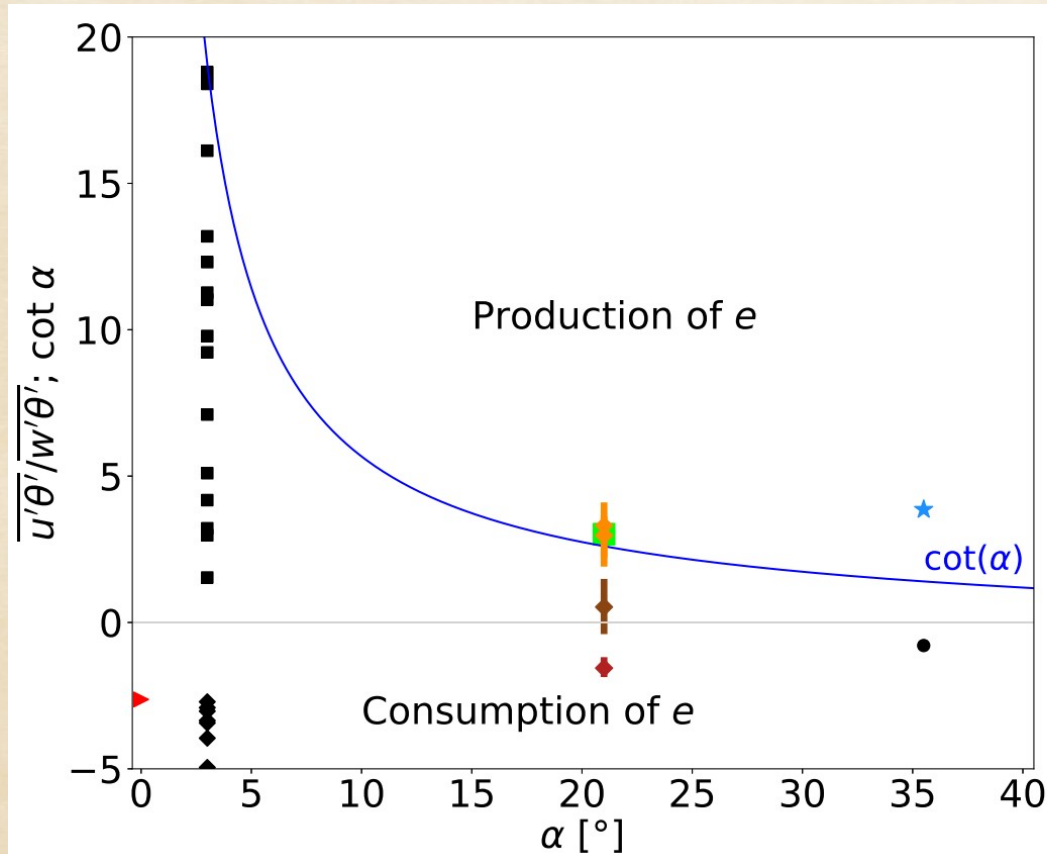
Weaker consumption

Enhanced consumption

Overview of the results from other field experiments

Limit between production and consumption of TKE by buoyancy

$$\frac{\overline{u' \theta'}}{\overline{w' \theta'}} = \cot(\alpha)$$



- Horst and Doran (1988), above jet peak. $N_p = 1$
- Grachev et al. (2016), above jet peak. $N_{p,i} = 1$
- ◆ Grachev et al. (2016), below jet peak. $N_{p,i} = 1$
- ▶ Wyngaard et al. (1971), flat terrain. $N_p = 27$
- ★ Oldroyd et al. (2016), above jet peak. $N_p = 495$
- Oldroyd et al. (2016), downslope wind. $N_p = 237$
- ◆ This study, above jet peak. $N_p = 15$
- ◆ This study, in the region of the maximum wind speed jet peak. $N_p = 15$
- ◆ This study, below jet peak. $N_p = 15$

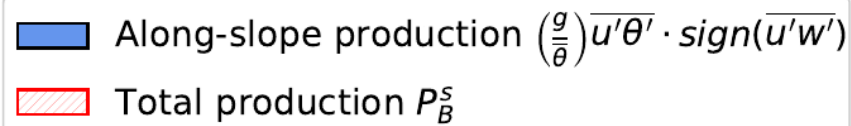
3

7

Buoyancy effect on turbulent shear stress $|\overline{u'w'}|$

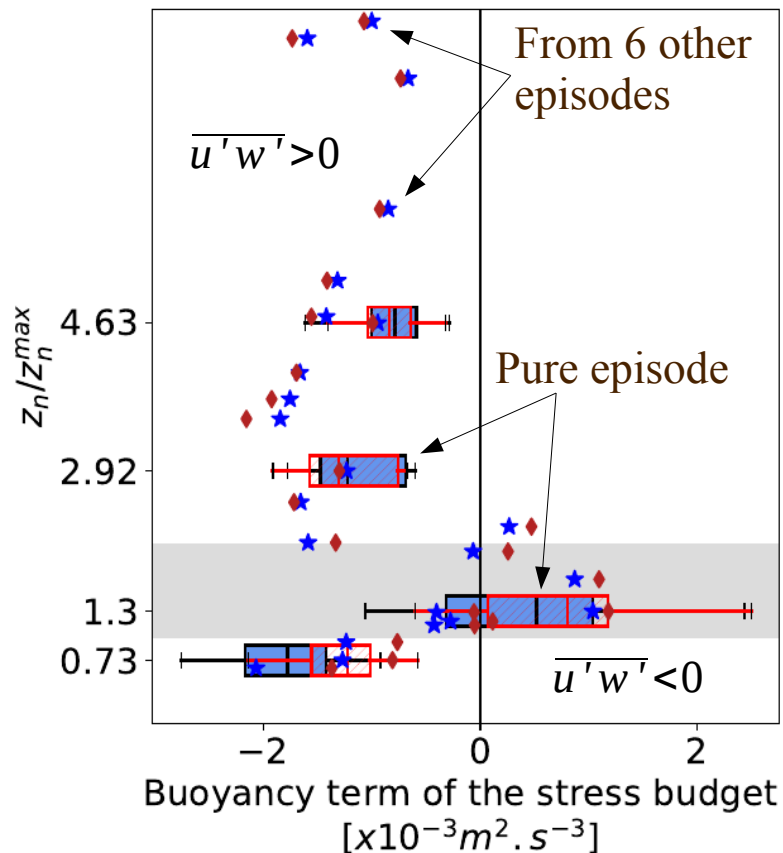
Buoyancy term in the turbulent shear stress budget

$$P_B^s \cdot \text{sign}(\overline{u'w'}) = \frac{g}{\theta} \cdot \overline{u_z' \theta'} = \frac{g}{\theta} \cdot (\overline{u' \theta'} \cos \alpha + \overline{w' \theta'} \sin \alpha)$$



Limited slope effect

Slope-normal height normalized by the maximum wind speed height



Consumption of turbulent shear stress $|\overline{u'w'}|$

Production of turbulent shear stress $|\overline{u'w'}|$

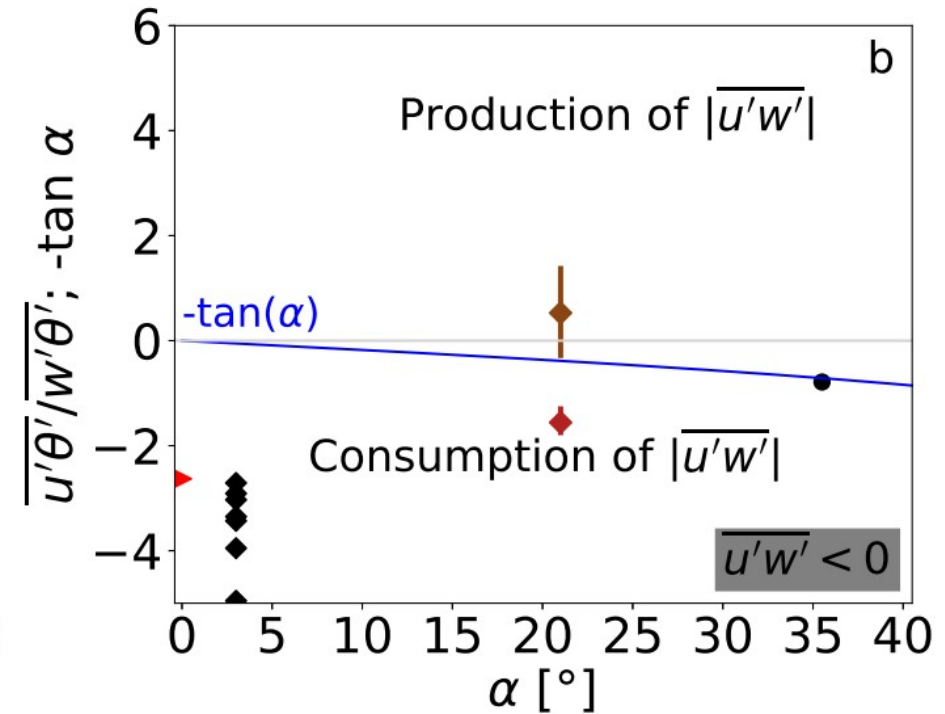
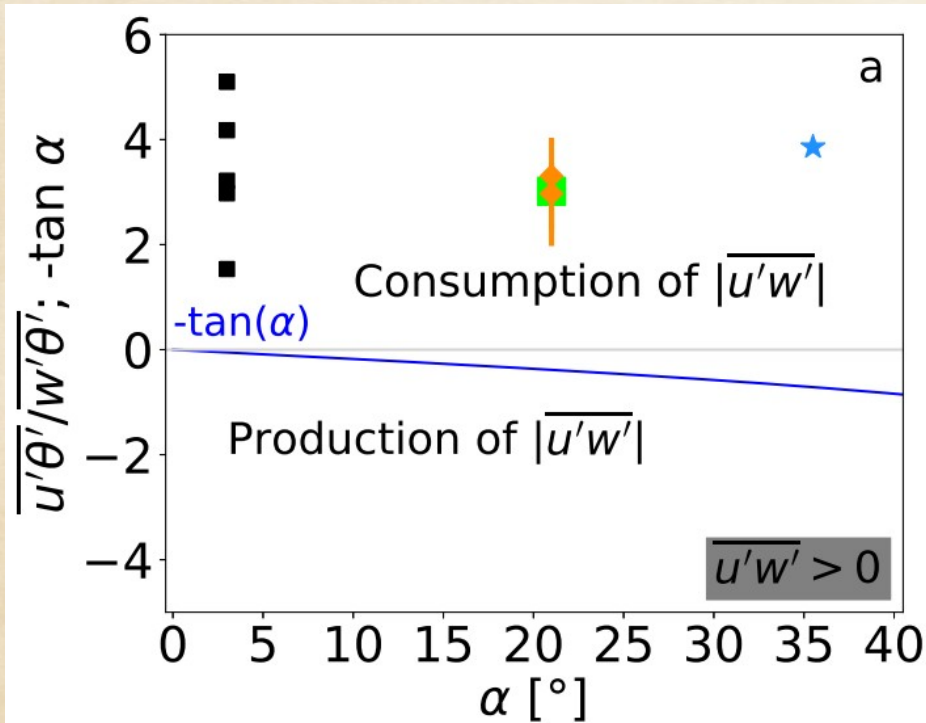
Consumption of turbulent shear stress $|\overline{u'w'}|$

Overview of the results from other field experiments

Limit between production and consumption of $\overline{u'w'}$ by buoyancy

$$\frac{\overline{u'\theta'}}{\overline{w'\theta'}} = -\tan(\alpha)$$

- Horst and Doran (1988), above jet peak. $N_p = 1$
- Grachev et al. (2016), above jet peak. $N_{p,i} = 1$
- ◆ Grachev et al. (2016), below jet peak. $N_{p,i} = 1$
- ▶ Wyngaard et al. (1971), flat terrain. $N_p = 27$
- ★ Oldroyd et al. (2016), above jet peak. $N_p = 495$
- Oldroyd et al. (2016), downslope wind. $N_p = 237$
- ◆ This study, above jet peak. $N_p = 15$
- ◆ This study, in the region of the maximum wind speed jet peak. $N_p = 15$
- ◆ This study, below jet peak. $N_p = 15$



1. Ill-defined external conditions

2. Lack of information in the inner layer of the jet, close to the ground

3. Streamline divergence/convergence



1. Tethered balloon up to 300m

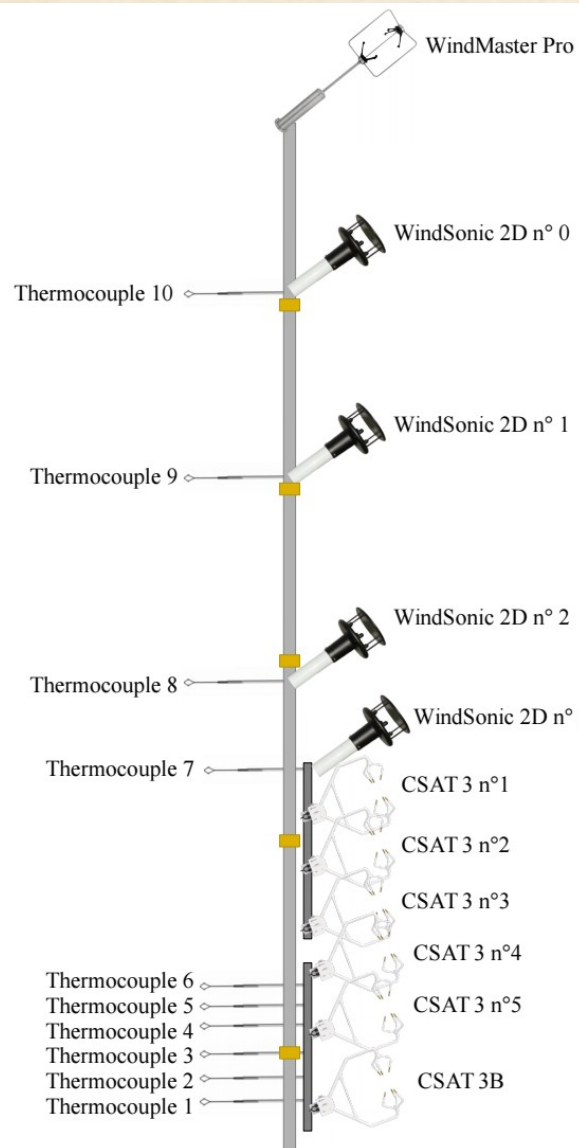
2. Cobra pitot-type probe: 3D velocity components for measurements close to the ground



3. 6 sonic anemometers to measure entrainment/detrainment in the lower part of the jet

A new field campaign from winter 2019

2019 February 12-28th



10m

- 11 wind speed levels
 - * 7 3D sonic anemometers (20Hz)
 - * 4 2D sonic anemometers (0.5Hz)
- 17 temperature levels (20Hz)
 - * 10 thermocouples
 - * 7 sonic anemometers

Meteorological mast:

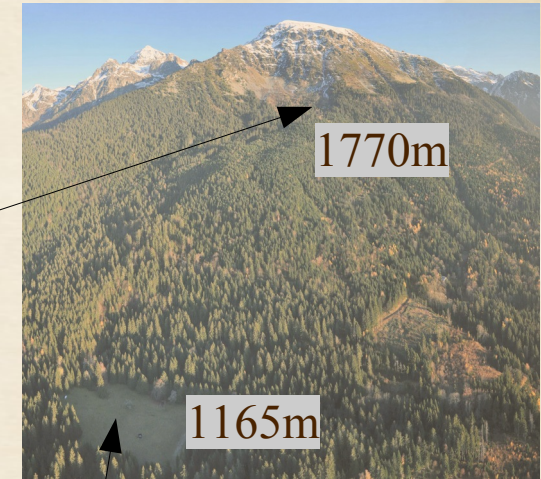
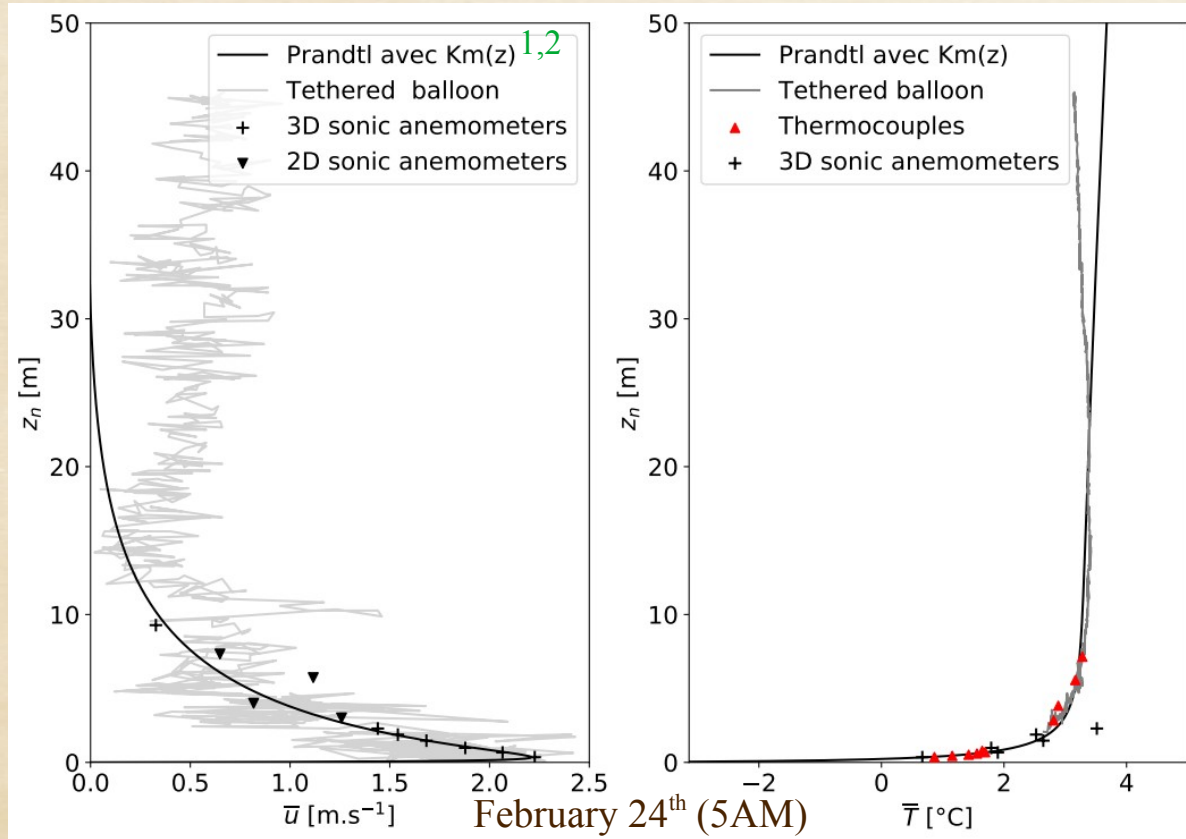
- Atmospheric pressure (CS100)
- Shortwave and longwave radiation fluxes (CNR1)
- Humidity and temperature (CS215)
- Distance sensor (SR50)



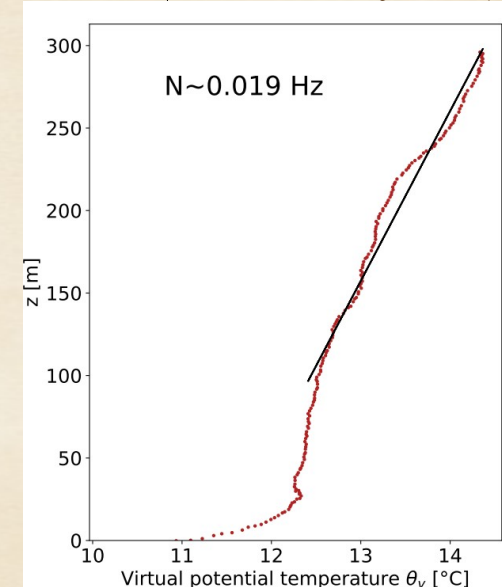
2019 dataset : improvements from the 2012 dataset

1. Tethered balloon:

- * Measurements above the mast: 10-50m
- * Background temperature stratification: up to 300m



February 15th (10AM)

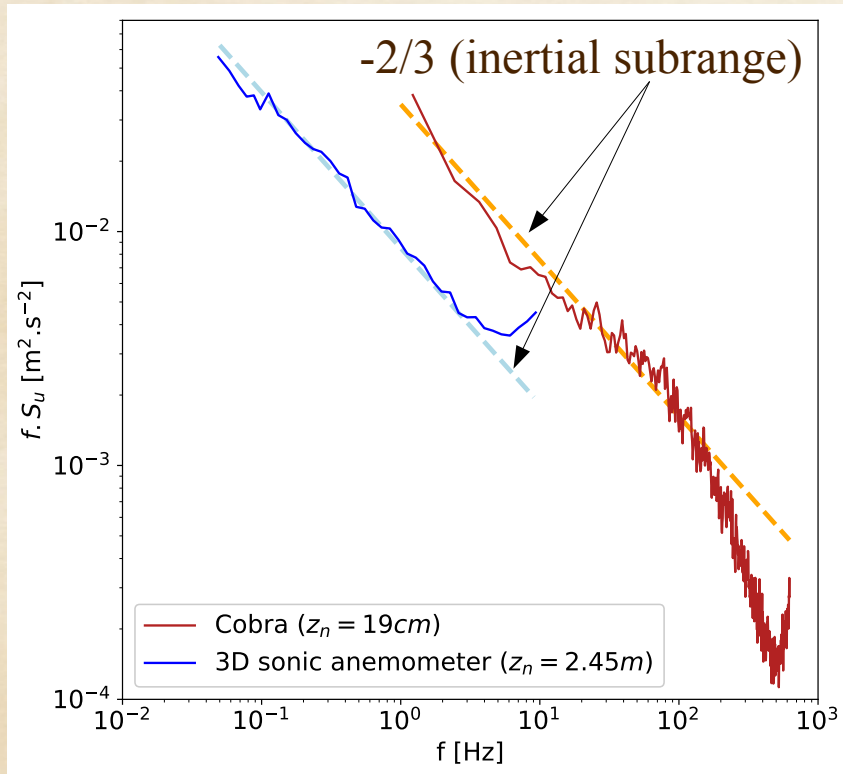


2019 dataset : improvements from the 2012 dataset

2. Cobra pitot-type probe : 3D velocity components

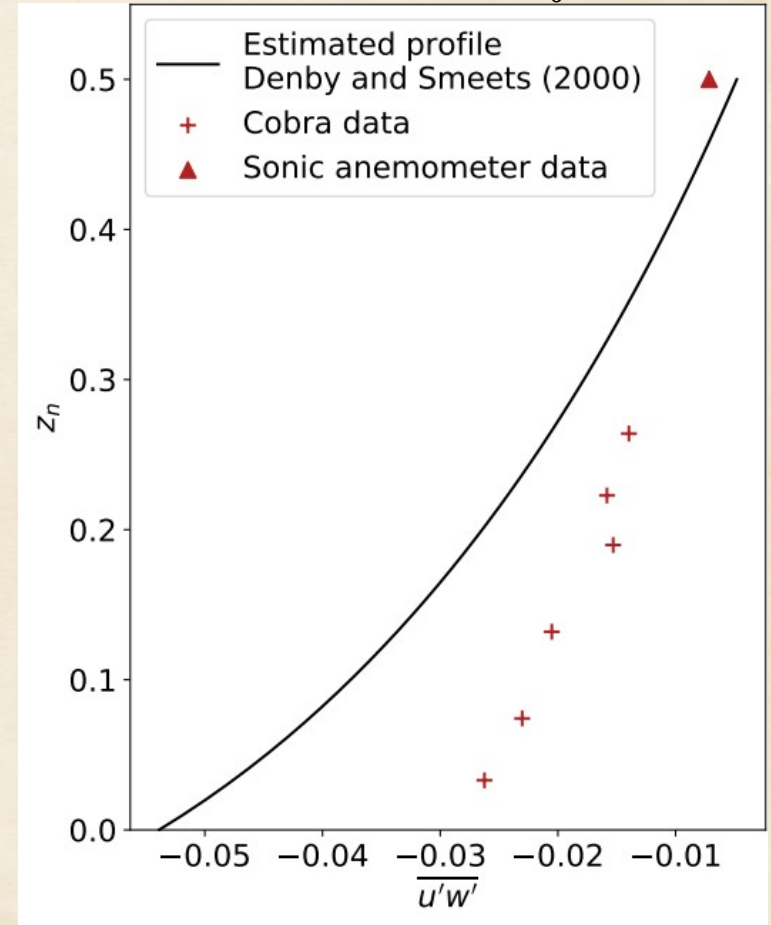
* $f = 1250$ Hz

* Level measurements : 4cm to 35cm



Streamwise velocity spectra with a well-developed inertial subrange

$$\overline{u'w'}(z_n) = \overline{u'w'}_0 - \sin(\alpha) \frac{g}{\theta_0} \int_{z_0}^{z_n} \theta(z_n) dz_n \quad 4$$



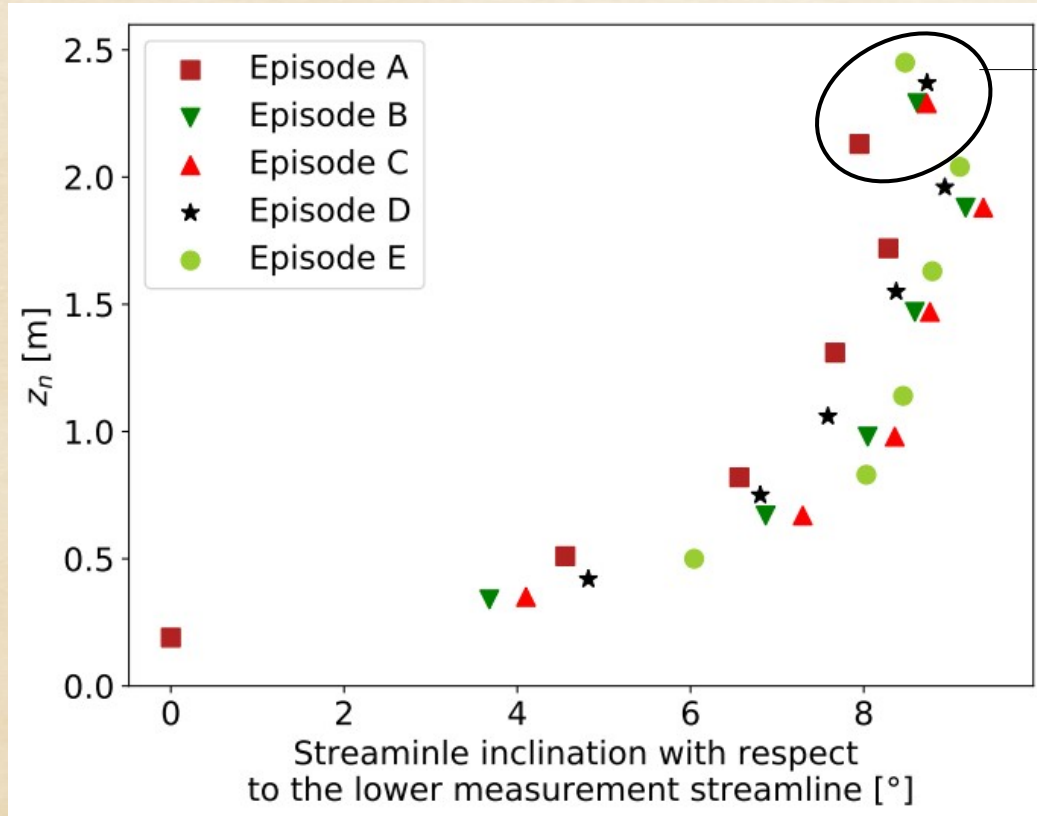
Turbulent shear stress variability along z_n close to the ground



2019 dataset : improvements from the 2012 dataset

3. Slope-normal entrainment/detrainment

- * Streamline inclination up to 9° with respect to the lower measurement level
- * Slope-normal velocity $W > 0$ in the lower part of the outer shear layer



→ Variability of measurement height due to melting/packing of the snow




2012 field experiment: buoyancy effects over steep slopes

- TKE production in the outer layer of the jet
- TKE consumption enhanced in the inner layer
- Consumption of turbulent shear stress (except around the maximum wind speed height)

→ Design of flux Richardson for TKE and stress Richardson for $\overline{u'w'}$

Charrondiere et al. (2020), *Boundary-Layer Meteorol* (Under review)

Design of the 2019 field experiment to complete the 2012 dataset



2019 field experiment: to dig further with these data

- Variability of turbulent shear stress close to the ground
- Presence of slope-normal velocity in the jet: entrainment/detrainment
- Energy spectra distribution close to the ground
- Buoyancy effects to reinforce conclusion from 2012 November dataset
- Full budget of TKE and turbulent shear stress:
 - * Buoyancy production/consumption
 - * Mechanical shear production/consumption
 - * Turbulent transport
 - * Vertical advection
 - * Dissipation

Cited references

Blein S (2016) *Observation and modelisation of stable atmospheric boundary layer in complex topography: turbulent processus of katabatic flow*. PhD thesis, Université Grenoble Alpes

Brun C, Blein S, Chollet J (2017) *Large-eddy simulation of a katabatic jet along a convexly curved slope. Part 1: statistical results*. J Atmos Sci 74(12):4047–4073

Charrondière C, Brun C, Sicart JE, Cohard JM, Biron R, Blein S (2020) *Buoyancy effects in the turbulence kinetic energy budget and Reynolds stress budget for a katabatic jet over a steep alpine slope*. Boundary-Layer Meteorol (Under review)

Denby B, Smeets C (2000) *Derivation of turbulent flux profiles and roughness lengths from katabatic flow dynamics*. Journal of applied Meteorology 39(9):1601–1612

Grisogono B, Oerlemans J (2001) *Katabatic flow: analytic solution for gradually varying eddy-diffusivities*. J Atmos Sci 58(21):3349–3354

Largeroy Y, Staquet C (2016) *Persistent inversion dynamics and wintertime PM10 air pollution in alpine valleys*. Atmospheric Environment 135:92–108

Oldroyd H, Pardyjak E, Higgins C, Parlange M (2016) *Buoyant turbulent kinetic energy production in steep-slope katabatic flow*. Boundary-Layer Meteorol 161(3):405–416

Whiteman CD (2000) *Mountain meteorology: fundamentals and applications*. Oxford University Press